Observation of subsurface monolayer thickness fluctuations in InGaN/GaN quantum wells by scanning capacitance microscopy and spectroscopy

X. Zhou and E. T. Yu[a)]
Department of Electrical and Computer Engineering, University of California, San Diego, La Jolla, California 92093-0407

D. Florescu, J. C. Ramer, D. S. Lee, and E. A. Armour
Veeco TurboDisc Operations, 394 Elizabeth Avenue, Somerset, New Jersey 08873

(Received 5 April 2004; accepted 19 May 2004)

Scanning capacitance microscopy and spectroscopy combined with numerical simulations have been used to image nanoscale electronic structures in $In_{0.30}Ga_{0.70}N/GaN$ quantum-well heterostructures grown by metalorganic chemical vapor deposition. Macroscopic capacitance–voltage spectroscopy and numerical simulations indicate that, depending on the bias voltage applied, either electron or hole accumulation in the *n*-type quantum-well region can occur. Scanning capacitance microscope images reveal local variations in electronic properties with structure similar to that of monoatomic steps observable in surface topography. Scanning capacitance spectroscopy combined with numerical simulations indicates that the observed features correspond to variations in carrier concentration arising from monolayer fluctuations in the thickness of the subsurface $In_{0.30}Ga_{0.70}N$ quantum-well layer, with thickness variations occurring over distances of tens of nanometers to a micron or more. © *2004 American Institute of Physics*. [DOI: 10.1063/1.1773358]

$In_xGa_{1-x}N/GaN$ quantum-well structures are of outstanding current interest for nitride semiconductor-based visible light emitters, including both light-emitting diodes and laser diodes.[1,2] Because of the high densities of point and extended defects in epitaxially grown nitride semiconductor material and the coupling that exists between structure and electronic properties via spontaneous and piezoelectric polarization effects, characterization and understanding of local, nanoscale structure and electronic properties in such devices are essential to achieve effective control over and optimization of device characteristics and performance.

We have used scanning capacitance microscopy (SCM) and spectroscopy[3,4] to characterize local, nanometer-scale electronic behavior in an $In_xGa_{1-x}N/GaN$ quantum-well structure. Macroscopic capacitance–voltage spectroscopy and numerical simulations are used to elucidate the basic mechanisms of local capacitance contrast, and suggest the occurrence, at different bias voltages, of either electron or hole accumulation within and near the $In_xGa_{1-x}N$ quantum-well layer. Scanning capacitance imaging and spectroscopy reveal the occurrence of carrier concentration variations at the nanoscale arising from a variety of sources including, most interestingly, monolayer fluctuations in $In_xGa_{1-x}N$ quantum-well thickness. The ability to image subsurface monolayer fluctuations in quantum-well layer thickness in this manner is particularly noteworthy given the difficulty of directly imaging subsurface electronic and structural properties in semiconductors at the atomic scale.

The sample employed in these studies, whose structure is illustrated schematically in Fig. 1, was grown by metalorganic chemical vapor deposition (MOCVD) on a *c*-plane sapphire substrate using a Veeco Turbodisc E300 GaNzilla platform. Following growth of 3000 Å of GaN with a donor concentration of $\sim 1\times10^{18}$ cm^{-3}, 120 Å GaN, a 30 Å $In_{0.30}Ga_{0.70}N$ quantum-well layer, and finally a 20 Å GaN capping layer were deposited. The $In_{0.30}Ga_{0.70}N$ quantum well and surrounding GaN layers were doped *n* type with a donor concentration in the mid-10^{16} cm^{-3} range, and the In concentration was determined based on the growth conditions employed. The very close proximity of the quantum-well structure to the sample surface enables high spatial resolution to be achieved since modulation of carriers in the quantum well is possible with only a small depletion layer width in the sample, and in addition improves sensitivity to quantum-well electronic structure since the tip–sample capacitance per unit area, being inversely proportional to the

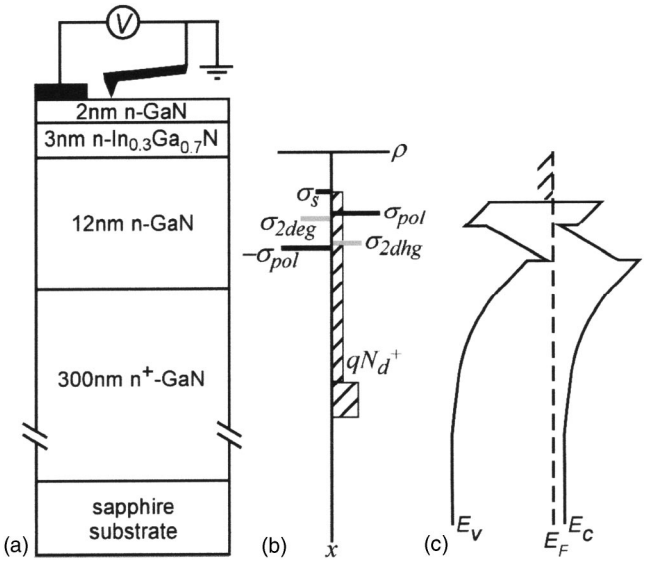

FIG. 1. (a) Schematic diagram of $In_{0.30}Ga_{0.70}N/GaN$ quantum-well sample structure. (b) Schematic diagram of the electrostatic charge distribution. Sheet charges corresponding to the two-dimensional electron gas (σ_{2deg}) and two-dimensional hole gas (σ_{2dhg}) are dependent on the bias voltage and therefore are indicated in gray. (c) Schematic energy-band-edge diagram for the $In_{0.30}Ga_{0.70}N/GaN$ quantum-well structure.

[a)]Electronic mail: ety@ece.ucsd.edu

depth of the quantum well below the surface, is very high.

All samples were cleaned with trichloroethylene, acetone, and methanol in an ultrasonic bath, followed by a rinse in isopropanol, prior to processing or imaging. Ohmic contacts were fabricated on all samples by deposition of 330 Å Ti/770 Å Al followed by annealing at 650 °C for 60 s. Circular Schottky contacts 125 μm in diameter were fabricated using 1000 Å Ni metallization and a standard lift-off process. Capacitance–voltage spectroscopy was performed using an HP 4285A precision low capacitance resonance (LCR) meter at ac bias frequencies ranging from 100 kHz to 1 MHz under ambient lighting conditions. Scanning capacitance microscopy and spectroscopy were performed in a Digital Instruments/Veeco Nanoscope IIIa Dimension 3100s scanning probe microscopy system using Co/Cr-coated tips with nominal tip radius of 25–50 nm.

To assist in the interpretation of scanning capacitance data, numerical simulations of capacitance–voltage spectra were performed using a one-dimensional Poisson–Schrödinger solver[5] with band offsets and polarization charge densities at the $In_{0.30}Ga_{0.70}N/GaN$ interfaces derived from experimentally measured values.[6] Briefly, four principal regimes of behavior were observed. For voltages greater than ~2 V applied to the Schottky contact, large capacitance due to carrier accumulation at the upper $In_{0.30}Ga_{0.70}N/GaN$ interface and in the top GaN layer is observed. For voltages near zero bias, carriers are depleted from the $In_{0.30}Ga_{0.70}N/GaN$ quantum-well structure and only a small depletion capacitance is present. As the bias voltage is decreased to values near −1 V, an increase in capacitance due to accumulation of holes at the lower $In_{0.30}Ga_{0.70}N/GaN$ interface is observed. Finally, at large negative bias voltages, hole accumulation at the upper $In_{0.30}Ga_{0.70}N/GaN$ interface and in the top GaN layer can occur, leading to a further increase in capacitance.

Figure 2 shows topographic and scanning capacitance images of the $In_{0.30}Ga_{0.70}N/GaN$ quantum-well sample structure for bias voltages of −2 to −3 V. Monolayer steps approximately 2.5–3 Å in height, indicative of step-flow growth, are clearly visible in the topographic image, as are pinned step edges terminated by screw-component dislocations.[7] With the probe tip biased at −2 V relative to the sample, little contrast is evident. At −2.25 V, small undulations are visible in the SCM image, and at −2.5 V these variations in contrast are much more evident with additional structural detail becoming clearly visible. At −3 V bias these features once again disappear. Based on our numerical simulations, we interpret the contrast in these images as arising from local variations in hole accumulation, induced by the negative bias applied to the tip, in or near the $In_{0.30}Ga_{0.70}N$ quantum well. We typically do not observe perturbations in carrier concentration near dislocations at these bias voltages; this is not unexpected as deep acceptor sites believed to be present in dislocations[8–10] would be unoccupied, and therefore uncharged, at bias voltages for which hole accumulation occurs in the $In_{0.30}Ga_{0.70}N$ quantum well.

The contrast observed in Fig. 2(d) is reminiscent of, although not identical to, the atomic step structure visible in Fig. 2(a). The latter point is reinforced in Fig. 3, which shows profiles of topography and of the scanning capacitance signal obtained simultaneously for a tip bias of −2.5 V. While the variations in scanning capacitance signal and in topography occur over similar length scales, there is not a one-to-one correspondence between specific topographic and scanning capacitance signal features. These observations suggest that the scanning capacitance signal contrast observed in this voltage range originates from features that are related to the surface atomic step structure present during

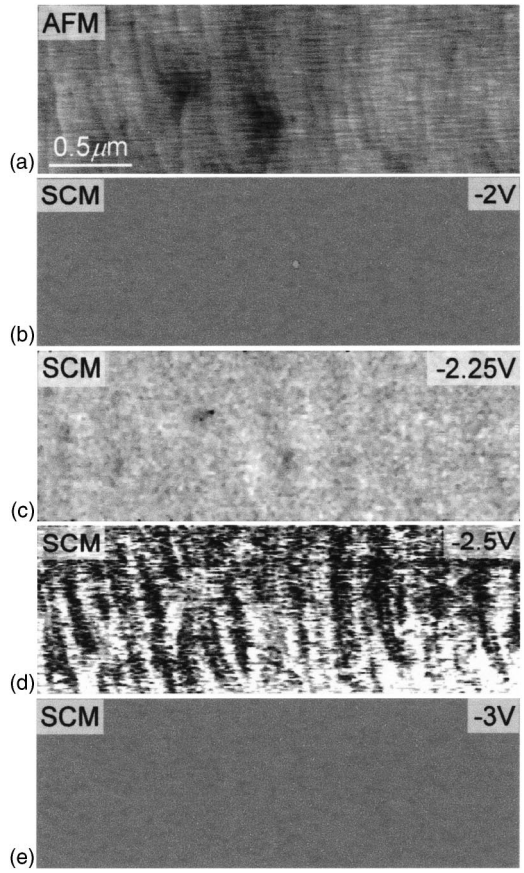

FIG. 2. (a) Topographic image and (b–e) scanning capacitance images of the $In_{0.30}Ga_{0.70}N/GaN$ quantum-well sample structure. Monoatomic steps as well as pinned step edges corresponding to threading dislocations are visible in the topographic image. A clear evolution in contrast revealing features corresponding to monolayer fluctuations in $In_{0.30}Ga_{0.70}N$ quantum-well thickness is apparent in the scanning capacitance images.

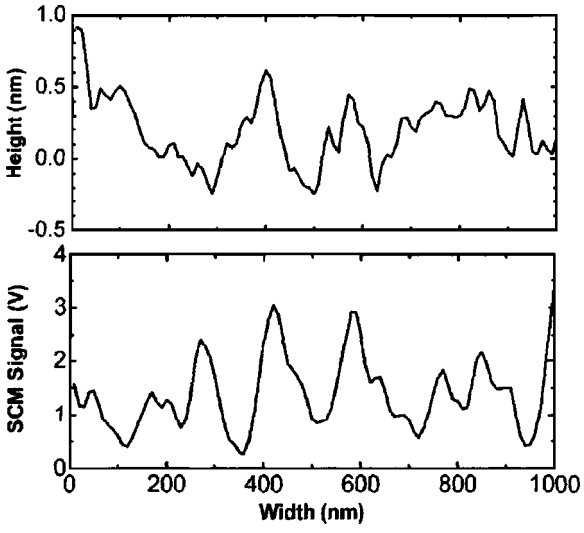

FIG. 3. Simultaneously obtained line scans of the (a) topographic height and (b) scanning capacitance signal revealing features in each that, while not exhibiting a one-to-one correlation, contain variations at similar length scales.

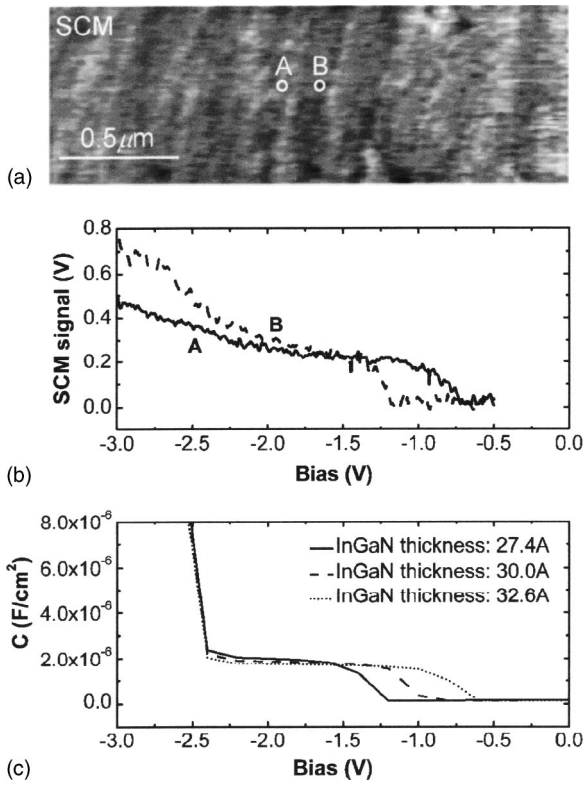

FIG. 4. (a) Scanning capacitance image obtained at a bias voltage of −2.5 V. (b) Scanning capacitance spectra obtained at points labeled A and B in (a). (c) Simulated capacitance–voltage spectra of $In_{0.30}Ga_{0.70}N$ quantum-well thicknesses of 30 Å plus or minus 1 monolayer. The experimental spectra and simulations suggest the locations marked A and B in the image are characterized by local quantum-well thicknesses that differ by 2 monolayers.

growth, while confirming that the contrast is not simply a topographic artifact.

Figure 4 shows a scanning capacitance image, local scanning capacitance spectra obtained at the locations indicated in the image, and numerically simulated capacitance–voltage curves for a Schottky contact to the $In_{0.30}Ga_{0.70}N/GaN$ sample structure shown in Fig. 1. The signal plotted is proportional to $|dC/dV|$, where C is the tip–sample capacitance. Both the simulation and the experimental data reveal an increase in capacitance with decreasing tip bias starting at approximately −0.5 to −1.5 V, which, based on the simulation results, we interpret as arising from accumulation of holes in the $In_{0.30}Ga_{0.70}N$ quantum well and, for more negative bias voltages, in the top GaN layer. Included in the simulation results plotted are curves for $In_{0.30}Ga_{0.70}N$ quantum-well thicknesses of 30, 27.4, and 32.6 Å, corresponding to the nominal quantum-well layer thickness plus or minus 1 monolayer. A variation in quantum-well thickness of 1 monolayer is seen to shift the threshold voltage for hole accumulation by ~0.3 V; similar variations in the thickness of the top GaN layer result in much smaller changes in threshold voltage. From the scanning capacitance spectra shown in Fig. 4, we see that the contrast observed in the image arises from a shift in threshold voltage for hole accumulation of approximately 0.6 V, in very good agreement with that predicted to arise from a 2 monolayer fluctuation in quantum-well thickness. It should be noted that voltages of −0.5 to −1.5 V shown in Figs. 4(b) and 4(c) correspond to bias voltages applied during SCM imaging of approximately −2 to −3 V. This discrepancy arises because the bias voltage during imaging is applied at each image point only for a duration of approximately 1–2 ms, while that applied during the spectroscopic measurement is ramped from −0.5 to −3.5 V at a frequency of ~1 Hz. As a result, the dynamics of charge trapping and detrapping and of hole accumulation in the $In_{0.30}Ga_{0.70}N$ quantum well are expected to differ in the two measurements, leading to a corresponding difference in threshold voltage for hole accumulation.

On this basis, we interpret the contrast visible in the SCM images shown in Figs. 2 and 4 as arising from monolayer fluctuations in the $In_{0.30}Ga_{0.70}N$ quantum-well layer thickness. In the samples studied here these fluctuations occur over length scales of several tens of nanometers in the direction normal to atomic step edges; however, regions of uniform quantum-well layer thickness can extend over a micron or more in the direction parallel to these step edges. Details of the structure and degree of monolayer fluctuations in quantum-well layer thickness will, of course, vary depending on the surface morphology present during epitaxial growth. However, the capability demonstrated here to image directly monolayer-level fluctuations in quantum-well layer thickness with nanoscale lateral resolution represents a powerful capability in characterization of such heterostructures for a variety of device applications.

In summary, we have used scanning capacitance microscopy and spectroscopy to characterize the local electronic structure in an $In_{0.30}Ga_{0.70}N/GaN$ quantum-well structure grown by MOCVD. On the basis of macroscopic capacitance–voltage measurements combined with numerical simulations, we see that either electron or hole accumulation can occur in the *n*-type quantum-well region. Scanning capacitance microscopy reveals image contrast with structure similar to that of monoatomic steps visible in atomic force microscopy topographic imaging of the sample surface. Comparison of nanoscale scanning capacitance spectroscopy measurements with numerical simulation indicates that the contrast observed in the SCM images arises from monolayer fluctuations in the thickness of the subsurface $In_{0.30}Ga_{0.70}N$ quantum-well layer.

Part of this work was supported by the NSF (Award No. ECS-0072912) and ONR (POLARIS MURI, Grant No. N00014-99-1-0729 monitored by Dr. Colin Wood).

[1] S. Nakamura and G. Fasol, *The Blue Laser Diode* (Springer, Berlin, 1997).
[2] S. Nakamura, M. Senoh, S.-i. Nagahama, N. Iwasa, T. Yamada, T. Matsushita, H. Kiyoku, Y. Sugimoto, T. Kozaki, H. Umemoto, M. Sano, and K. Chocho, Appl. Phys. Lett. **72**, 211 (1998).
[3] K. V. Smith, E. T. Yu, J. M. Redwing, and K. S. Boutros, Appl. Phys. Lett. **75**, 2250 (1999).
[4] D. M. Schaadt, E. J. Miller, E. T. Yu, and J. M. Redwing, Appl. Phys. Lett. **78**, 88 (2001).
[5] G. L. Snider, computer program 1D Poisson/Schrődinger: A band diagram calculator, University of Notre Dame, Notre Dame, IN (1995).
[6] H. Zhang, E. J. Miller, E. T. Yu, C. Poblenz, and J. S. Speck, Appl. Phys. Lett. **84**, 4644 (2004).
[7] B. Heying, E. J. Tarsa, C. R. Elsass, P. Fini, S. P. DenBaars, and J. S. Speck, J. Appl. Phys. **85**, 6470 (1999).
[8] A. F. Wright and U. Grossner, Appl. Phys. Lett. **73**, 2751 (1998).
[9] J. Elsner, R. Jones, M. I. Heggie, P. K. Stitch, M. Haugk, Th. Frauenheim, S. Őberg, and P. R. Briddon, Phys. Rev. B **58**, 12571 (1998).
[10] B. S. Simpkins, E. T. Yu, P. Waltereit, and J. S. Speck, J. Appl. Phys. **94**, 1448 (2003).